

Electronic Supplementary Information (ESI)

Graphene Aerogel Supported Crystalline ZnO@Amorphous Zn₂GeO₄ Core–Shell Hierarchical Structure for Lithium Storage

Meng Jiang^a, Tengfei Zhou^{b*}, Wei Liu^a, Chuanqi Feng^a, Jianwen Liu^a, Zaiping Guo^{ab*}

^aHubei Collaborative Innovation Center for Advanced Organic Chemical Materials, Ministry-of-Education Key Laboratory for Synthesis and Applications of Organic Functional Molecules, Hubei University, Wuhan 430062, China

^bInstitute for Superconducting and Electronic Materials, School of Mechanical, Materials, and Mechatronics Engineering, University of Wollongong, North Wollongong, NSW 2500, Australia

Experiment

Synthesis of Na₂GeO₃ solution

0.5300g Na₂CO₃ (Aladdin, AR) and 0.5230g GeO₂ (Aladdin 99.999% 200 mesh) were mixed and annealed at 900°C for 12 h. Then, the product was dissolved in 50 mL deionized (DI) water to make a transparent solution of Na₂GeO₃ hydrates (0.1 M).

Synthesis of ZZGO/GA composite

Graphene oxide (GO) was synthesized via the modified Hummer's method.^[16] 60.0 mg GO was dispersed in 20 ml DI water to form a 3 mg/ml homogeneous solution. Then, 0.4390 g Zn(AC)₂·2H₂O (Aladdin, 99.99%), 0.3522 g vitamin C (Sinopharm, AR), and 10 mL as-prepared Na₂GeO₃ solution were added into the GO solution and kept under stirring for 30 min. The solution was kept at 80°C for 6 h. After cooling down naturally, the as-prepared composite was washed with DI water. The product was prepared by freeze-drying the composite.

Synthesis of pure Zn₂GeO₄ (ZGO)

0.4390 mg Zn(AC)₂·2H₂O and 0.1046 g GeO₂ powder were dissolved in 30 mL DI water, with stirring for 30 min. The mixture was transferred into a 50 mL Teflon-lined autoclave and heated at 180°C for 24 h. The collected white precipitates were washed with DI water and ethanol several times and dried at 80°C for 6 h.

Synthesis of amorphous ZGO (A-ZGO)

0.4390 g Zn(AC)₂·2H₂O was dissolved in 50 mL DI water. The obtained 10 ml Na₂GeO₃ solution was added dropwise to the Zn(AC)₂ solution, and white precipitates were formed immediately. The mixture was stirred for 30 min at room temperature.

The collected white precipitates were washed with DI water and ethanol several times and dried at 80°C for 6 h.

Electrochemical measurements

The electrodes were fabricated by mixing the active material, Super P, and Na-carboxymethyl cellulose (CMC) in a weight ratio of 8:1:1 in deionized water, followed by pasting the slurry onto copper foil by scraping with a knife. After drying in vacuum at 80 °C for 24 h, the electrode was cut into small pieces with a diameter of 8 mm for use as working electrodes in 2032 coin cells. The coin cells were then assembled in an argon filled glove box, using lithium metal as the counter electrode, Celgard 2300 membrane as the separator, and 1 M LiPF₆ dissolved in ethylene carbonate, diethyl carbonate, and dimethyl carbonate (EC-DEC-DMC) mixed solvent (1:1:1 by weight) as the electrolyte. The electrochemical performances were recorded on a Land battery measurement system (Wuhan, China) with a cut-off voltage of 0.01–2.80 V vs. Li/Li⁺ at room temperature. Cyclic voltammetry (CV) curves were recorded on an electrochemical workstation (CHI 660d) at a scan rate of 0.1 mV s⁻¹ between 0.01 and 2.80 V.

Characterization

The as-prepared material was characterized by X-ray diffraction (XRD) with Cu K α radiation at a scanning rate of 5° min⁻¹ (D/MAX-IIIC, Rigaku, Japan). The morphologies and particle sizes of the samples were investigated by field emission scanning electron microscopy (SEM, JEOL JSM-7500FA) and field emission transmission electron microscopy (FTEM; Tecnai G2 F30). X-ray photoelectron

spectroscopy (XPS) was conducted on an ESCALAB 250Xi photoelectron spectrometer using monochromatic Al K α radiation under vacuum at 2×10^{-6} Pa. All of the binding energies were referenced to the C 1s peak at 284.8 eV of the surface adventitious carbon. Raman analysis was performed with a Raman spectrometer (Renishaw plc, Wotton-under-Edge, UK). The thermal properties of the as-prepared samples were characterized by thermogravimetric analysis (TGA; DIAMOND TG/DTA, PERKIN ELMER, USA) under air over a temperature range of 30–800 °C with a ramp rate of 20 °C min⁻¹. Fourier transform infrared spectroscopy (FT-IR) was conducted on a MAGNA-IR 750 (NICOLET iS10, USA).

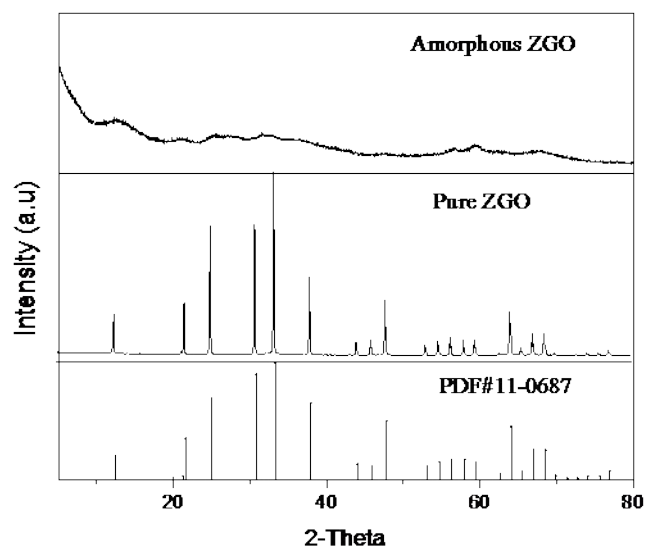


Figure S1 X-ray diffraction patterns of pure ZGO and amorphous ZGO.

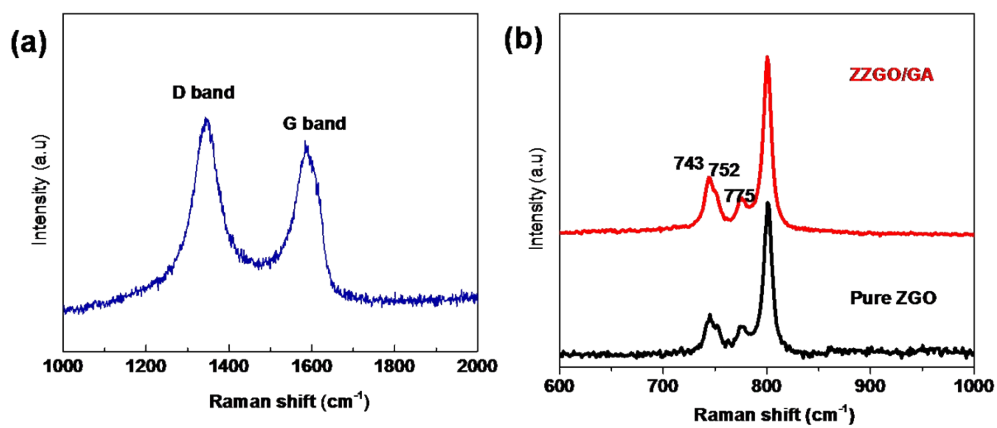


Figure S2 (a) Raman spectra of ZZGO/GA. (b) Raman spectra of ZZGO/GA and pure ZGO.

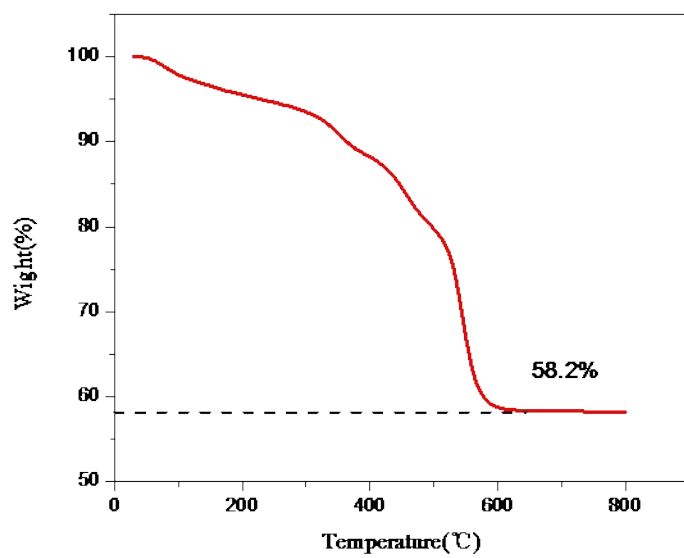


Figure S3 TGA curve of ZZGO/GA nanocomposites

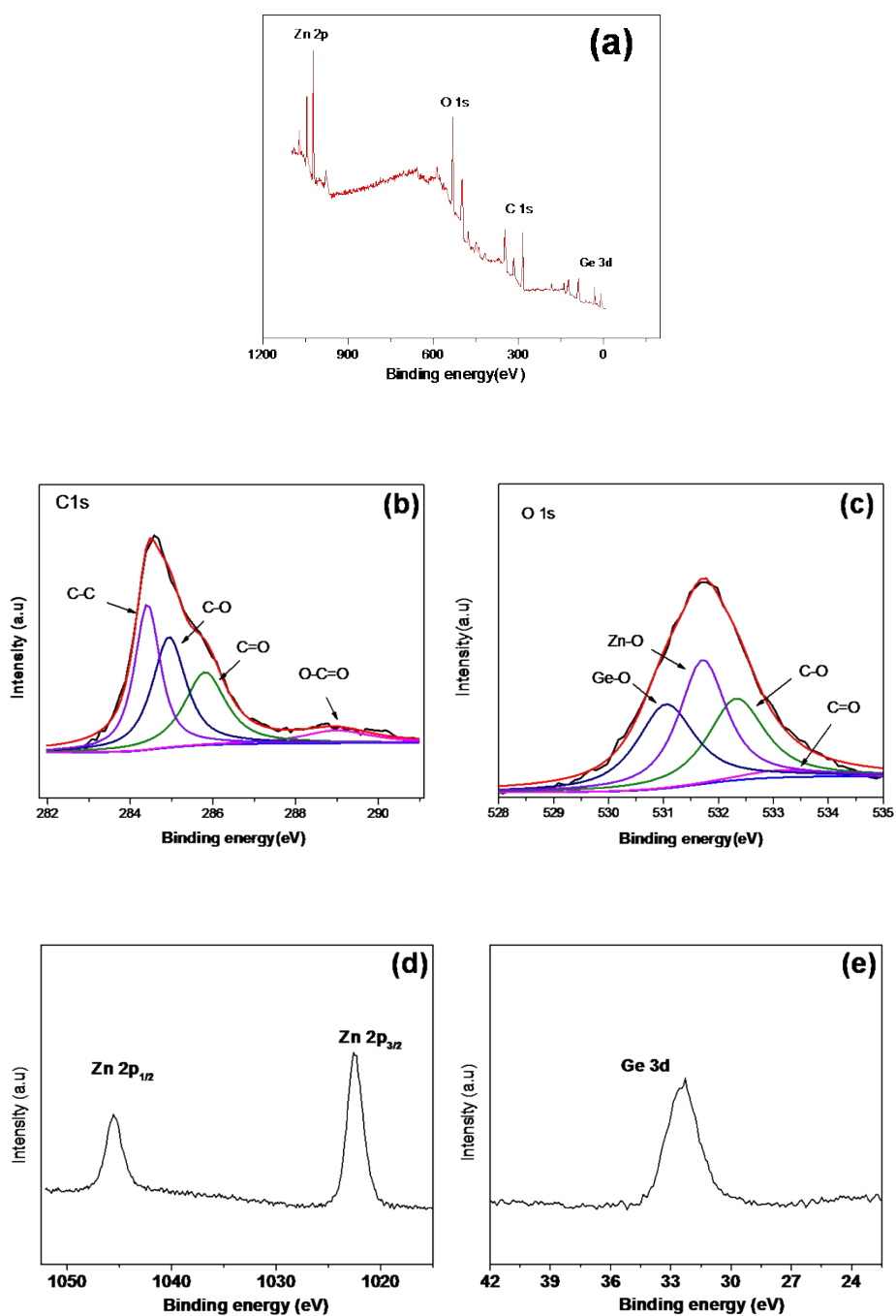


Figure S4 (a) XPS survey spectrum (b) the C1s and (c) O1s (d) Zn_{2p}, (e) Ge_{3d} spectra of ZZGO/GA.

The XPS spectrum of C 1s (Figures 3.b) could be deconvoluted into four peaks (centered at 284.4, 284.9, 285.8, and 288.9 eV), which corresponded to reference C=C, C-O, C=O, and O=C-O, respectively.^[1]

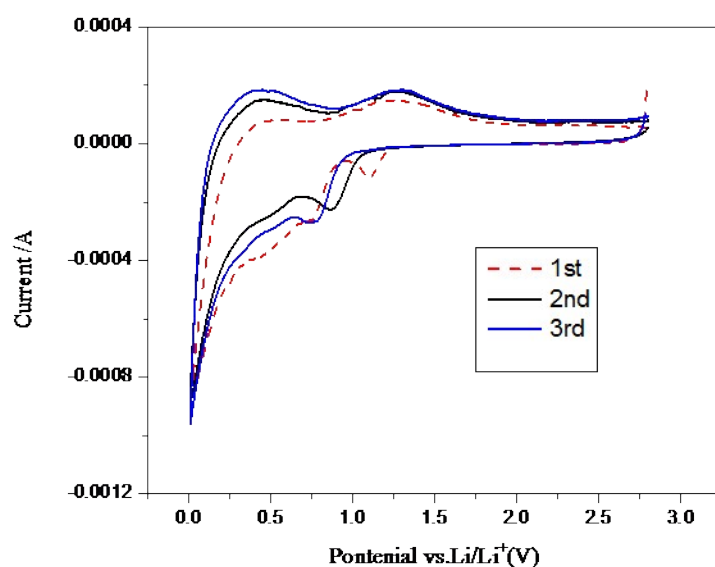
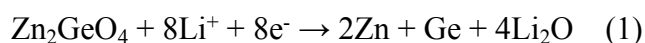


Figure S5 CV spectra of ZZGO/GA electrode with the potential window from 0.01 V to 2.80 V.

In the first cathodic process (discharge process), two sharp peaks at 0.75 could be attributed to a multiple electrochemical reaction process, which included the formation of solid electrolyte interface (SEI) layers and the decomposition of Zn_2GeO_4 into Zn, Ge, and Li_2O . At lower potentials, a pronounced anodic peak that started at 0.25 V could be assigned to the alloy reactions of Li-Zn, Li-Ge and Li-C.^[2] During the anodic potential sweeps, two broad oxidation peaks at 0.4 V and 1.4 V were observed, which were associated with the delithiation of Li-Zn and Li-Ge, followed by the partial oxidation of Zn and Ge.^[3] The enhancement of oxidation peak at 0.4V indicated that the capacity increasing was possibly related to the slow activation process of alloying and redox reaction of Zinc lithiation/delithiation. And the overall electrochemical reaction that occurs during Li insertion and extraction could be described according to Equations (1) - (6).^{[4][5]}





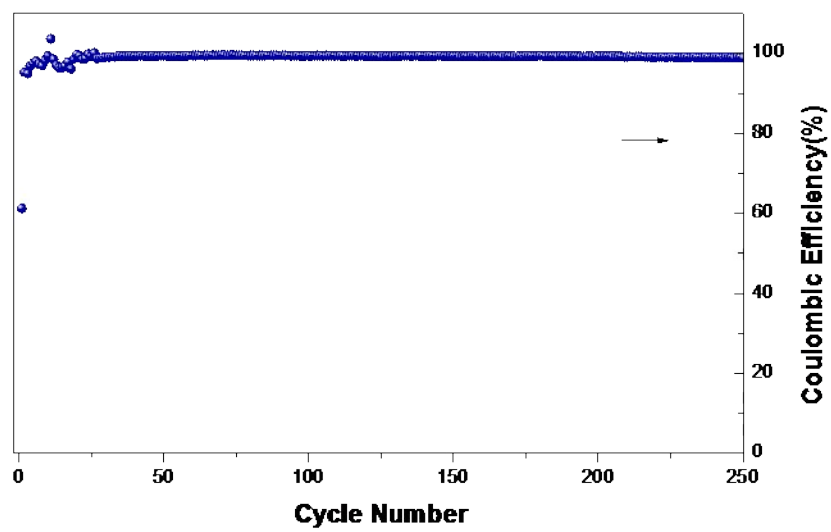


Figure S6 Coulombic efficiency of ZZGO/GA.

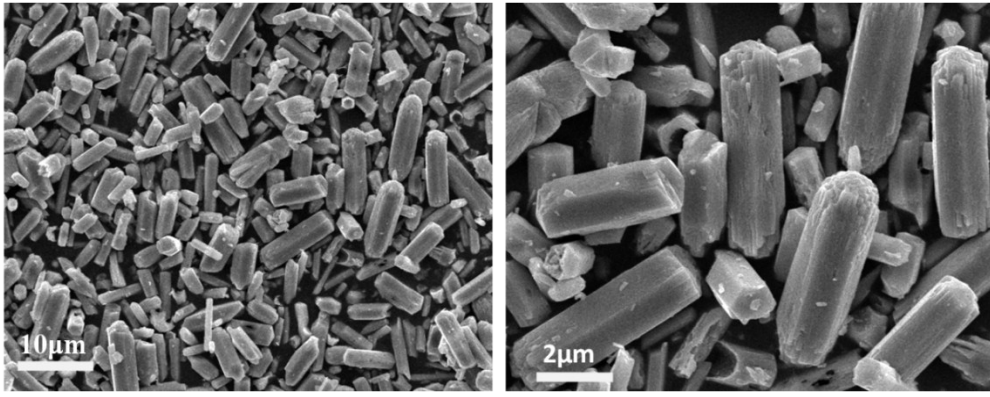


Figure S7 SEM images of pure ZGO at low and high magnification.

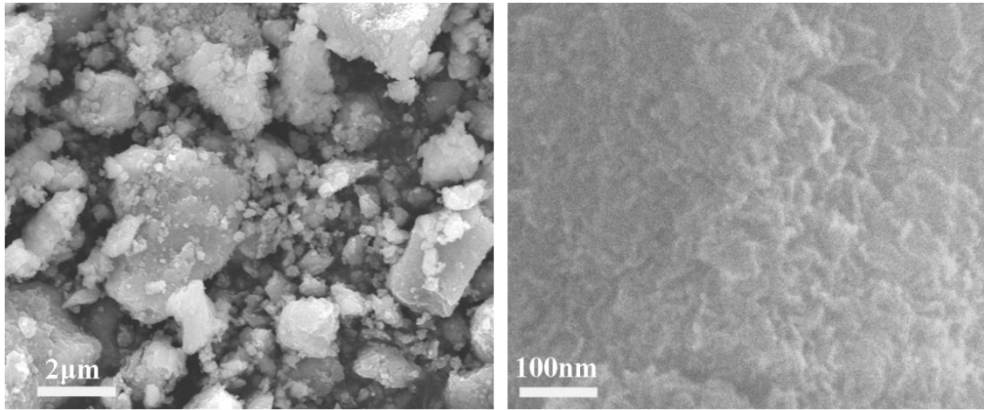


Figure S8 SEM images of A-ZGO at low and high magnification.

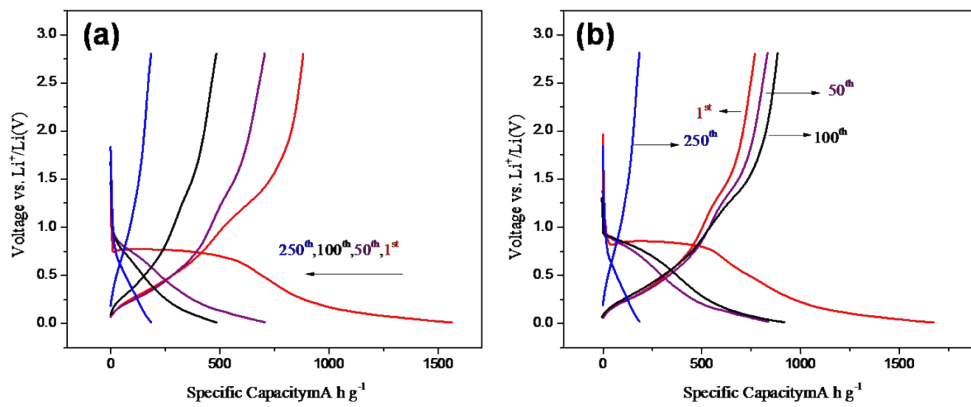


Figure S9 discharge-charge potential profiles of (a) pure ZGO and (b) A-ZGO.

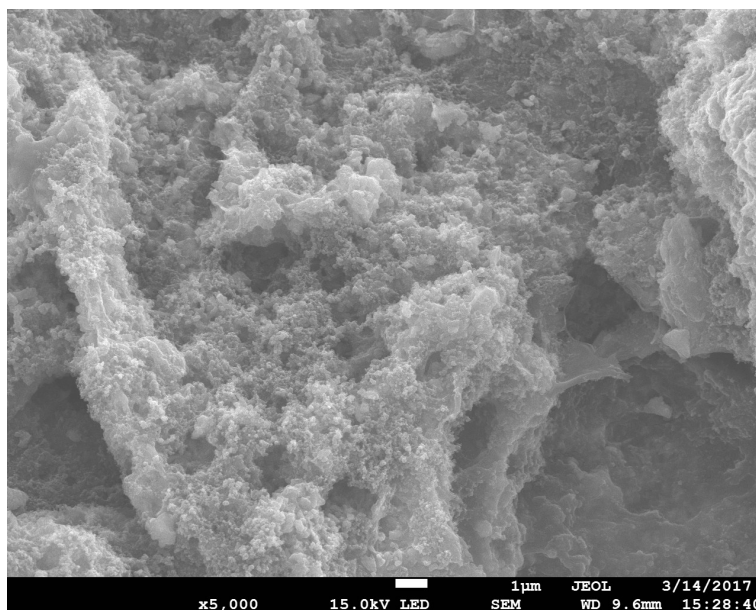


Figure S10. Typical SEM images of ZnO@Amorphous Zn₂GeO₄ electrode after 200 cycles at the current density of 500 mA g⁻¹.

References

- [1] Y. Zhou, Q. Liu, D. B. Liu, H. Xie, G. X. Wu, W. F. Huang, Y. F. Tian, Q. He, A. Khalil, Y. A. Haleem, T. Xiang, W. S. Chu and C. W. Zou, L. Song, *Electrochimica Acta*, 2015, **173**, 8.
- [2] F. Zou , X. Hu , Y. Sun , W. Luo , F. Xia , L. Qie , Y. Jiang and Y. Huang , *Chem. Eur. J.*, 2013 , **19** , 6027.
- [3] X. D. Li , Y. Feng, M. C. Li , W. Li , H. Wei and D. D. Song, *Adv. Funct. Mater.*, 2015, **25**, 6858.
- [4] R. Yia, J. K. Feng, D. P. Lv, M. Gordin, S. R. Chen, D. Choi and D. H. Wang, *Nano Energy*, 2013, **2**, 498.
- [5] S. M. Abbas, S. T. Hussain, S. Ali, N. Ahmad, N. Ali and S. Abbas, *J. Mater. Sci.*, 2013, **48**, 5429.